View metadata, citation and similar papers at core.ac.uk

brought to you by CORE

provided by Electronic Publication Information Center

Harmful Algae 55 (2016) 56–65

Contents lists available at ScienceDirect

Harmful Algae

journal homepage: www.elsevier.com/locate/hal

Review

Morphology, molecular phylogeny and azaspiracid profile of *Azadinium poporum* (Dinophyceae) from the Gulf of Mexico

Zhaohe Luo [a,b], Bernd Krock [c,*], Kenneth Neil Mertens [d,1], Andrea Michelle Price [e], Robert Eugene Turner [f], Nancy N. Rabalais [g], Haifeng Gu [b,*]

[a] College of Life Science and Technology, Jinan University, Guangzhou 510632, China
[b] Third Institute of Oceanography, SOA, Xiamen 361005, China
[c] Alfred Wegener Institute for Polar and Marine Research, Am Handelshafen 12, D-27570 Bremerhaven, Germany
[d] Research Unit for Palaeontology, Ghent University, Krijgslaan 281 S8, 9000 Ghent, Belgium
[e] Department of Geography, McGill University, Burnside Hall, 805 Sherbrooke Street West, Montreal, QC, Canada H3A OB9
[f] Department of Oceanography and Coastal Sciences, Louisiana State University, Baton Rouge, LA 70803, USA
[g] Louisiana Universities Marine Consortium, Chauvin, LA 70344, USA

ARTICLE INFO

Article history:
Received 1 September 2015
Received in revised form 9 February 2016
Accepted 9 February 2016
Available online

Keywords:
AZA-2
AZA-2 phosphate
Biogeography
LC–MS/MS
LSU rDNA
Ribotype D

ABSTRACT

Azadinium poporum produces a variety of azaspiracids and consists of several ribotypes, but information on its biogeography is limited. A strain of *A. poporum* (GM29) was incubated from a Gulf of Mexico sediment sample. Strain GM29 was characterized by a plate pattern of po, cp, x, 4′, 3a, 6″, 6C, 5S, 6‴, 2⁗, a distinct ventral pore at the junction of po and the first two apical plates, and a lack of an antapical spine, thus fitting the original description of *A. poporum*. The genus *Azadinium* has not been reported in waters of the United States of America before this study. Molecular phylogeny, based on large subunit ribosomal DNA (LSU rDNA) and internal transcribed spacer (ITS) sequences, reveals that strain GM29 is nested within the well-resolved *A. poporum* complex, but forms a sister clade either to ribotype B (ITS) or ribotype C (LSU). It is, therefore, designated as a new ribotype, termed as ribotype D. LSU and ITS sequences similarity among different ribotypes of *A. poporum* ranges from 95.4% to 98.2%, and from 97.1% to 99.2% respectively, suggesting that the LSU fragment is a better candidate for molecular discrimination. Azaspiracid profiles were analyzed using LC–MS/MS and demonstrate that strain GM29 produces predominantly AZA-2 with an amount of 45 fg/cell. The results suggest that *A. poporum* has a wide distribution and highlights the risk potential of azaspiracid intoxication in the United States.

© 2016 Elsevier B.V. All rights reserved.

Contents

1. Introduction . . . 57
2. Materials and methods . . . 57
 2.1. Sample collection and treatment . . . 57
 2.2. Light microscopy (LM) . . . 57
 2.3. Scanning electron microscopy (SEM) . . . 57
 2.4. PCR amplifications and sequencing . . . 58
 2.5. Sequence alignment and phylogenetic analysis . . . 58
 2.6. Chemical analysis of azaspiracids . . . 58
  2.6.1. Single reaction monitoring (SRM) measurements . . . 58
  2.6.2. Precursor ion experiments . . . 59
  2.6.3. Collision Induced Dissociation (CID) spectra . . . 59

* Corresponding authors.
E-mail addresses: bernd.krock@awi.de (B. Krock), guhaifeng@tio.org.cn (H. Gu).
[1] Now at: Ifremer, LER BO, Station de Biologie Marine, Place de la Croix, BP40537, F-29185 Concarneau Cedex, France.

http://dx.doi.org/10.1016/j.hal.2016.02.006
1568-9883/© 2016 Elsevier B.V. All rights reserved.

3. Results . . . 59
3.1. Morphology . . . 59
3.2. Molecular analysis and phylogeny . . . 59
3.3. AZA profile . . . 59
4. Discussion . . . 61
4.1. Morphology and biogeography . . . 61
4.2. Phylogeny and genetic differentiation . . . 64
4.3. Toxin profiles . . . 64
5. Conclusions . . . 64
Acknowledgements . . . 64
References . . . 64

1. Introduction

The known diversity of the dinophyte genus *Azadinium* Elbrächter and Tillmann has increased rapidly. Up to ten species have been described in the past five years (Tillmann et al., 2009, 2010, 2011, 2014; Luo et al., 2013; Percopo et al., 2013). Additionally, *Amphidoma caudata* Halldal has been transferred to *Azadinium* based on both morphology and molecular phylogeny (Nézan et al., 2012). The genus *Azadinium* was characterized by a plate pattern of po, cp, x, 3-4′, 2-3a, 6″, 6C, 5S, 6‴, 2⁗ (Tillmann et al., 2009; Luo et al., 2013), in which the presence of anterior intercalary plates and a canal plate resembles the Peridiniales and the presence of six precingular and postcingular plates resembles the Gonyaulacales. In the molecular phylogeny, the genus *Azadinium* is monophyletic and forms an independent lineage together with *Amphidoma* Stein, which is classified within the family Amphidomataceae, but its higher level designation remains to be determined (Tillmann et al., 2012a, 2014).

Most *Azadinium* species were described from samples collected in European waters, but that does not mean that there is a restricted distribution of these small dinoflagellates. For example, *Azadinium spinosum* was also reported in the Mexican Pacific (Hernández-Becerril et al., 2012), and *Azadinium poporum* was found in Korea (Potvin et al., 2011), China (Gu et al., 2013), New Zealand (Smith et al., 2015) and Argentina (Tillmann et al., 2016). *Azadinium* diversity might be underestimated because their cells are rather small and molecular detection is not routinely carried out (Toebe et al., 2013).

The type species of *Azadinium* (*A. spinosum*) was related to azaspiracids (AZA-1 and AZA-2) and thus was the organism responsible for cases of human intoxication via mussel consumption (Tillmann et al., 2009). Later, two other species (*Azadinium dexteroporum*, *Azadinium poporum*) were found to contain AZAs too (Percopo et al., 2013; Gu et al., 2013; Krock et al., 2014). It is worth noting that *A. poporum* comprises several genetically different ribotypes that are morphologically identical. The strains from Europe and New Zealand share identical sequences and belong to ribotype A, whereas those from Korea, China and Argentina belong to ribotype B or C (Gu et al., 2013; Smith et al., 2015; Tillmann et al., 2016). Additional ribotypes can be expected to be discovered because only a limited number of *A. poporum* strains have been sequenced.

The presence of azaspiracids (AZA) has been reported in mussels of northern Africa (Taleb et al., 2006), mussels from northern Europe (Satake et al., 1998), scallops and mussels from Chile (Lopez-Rivera et al., 2010), a marine sponge from Japan (Ueoka et al., 2009), shellfish from China (Yao et al., 2010), shellfish from New Zealand (Smith et al., 2015) and plankton samples from the Pacific coast of the USA (Trainer et al., 2013). However, AZA producing species have not been reported in some of these areas, e.g., from the USA. Incubated sediment samples from the northern Gulf of Mexico, generated one strain of *Azadinium poporum*. Its morphology was examined in detail, and its partial large subunit ribosomal DNA (LSU rDNA) and internal transcribed spacer regions (ITS) sequences were determined. This strain was also grown in larger quantities and analyzed for the presence of AZAs.

2. Materials and methods

2.1. Sample collection and treatment

A box core was collected from the northern Gulf of Mexico (29.3250° N, 93.4167° W, water depth: 17.3 m) on August 1, 2014. The top 2 cm were sliced off and stored in the dark at 4 °C until further treatment. Approximately 5 g of wet sediment was mixed with 20 mL of filtered sea water and sonicated for 2 min (100 W) to dislodge detrital particles. The watery slurry was incubated directly in a series of small containers in f/2-Si medium (Guillard and Ryther, 1962) at 20 °C, 90 $\mu E\ m^{-2}\ s^{-1}$ under a 12:12 h light:dark cycle (hereafter called "standard culture conditions"). *Azadinium* cells are characterized by swimming at low speed, interrupted by short, high-speed 'jumps' in various directions (Tillmann et al., 2009). Cells exhibiting such a characteristic swimming behavior were isolated by means of drawn-out Pasteur pipettes and established in clonal cultures. Only one strain (GM29) was established from one container, and it was maintained under standard culture conditions.

2.2. Light microscopy (LM)

Live cells were examined under a Zeiss Axio Imager microscope (Carl Zeiss, Göttingen, Germany) equipped with both differential interference illumination and epifluorescence. Light micrographs were obtained using a Zeiss AxiocamHRc digital camera. Approximately 1 mL of live, healthy culture in mid exponential growth phase was transferred to a 1.5 mL microcentrifuge tube, and stained with 1:100,000 Sybr Green (Sigma–Aldrich, St. Louis, USA) for 10 min. The cells were viewed and photographed through a Zeiss Filterset (excitation BP 450–490; beamsplitter FT 510; emission LP 515). Cells in mid-exponential growth phase were fixed with 5% Lugol's solution and cell sizes were measured at 400× magnification. Thirty cells were measured for the strain GM29.

2.3. Scanning electron microscopy (SEM)

Mid-exponential batch cultures were collected by centrifugation at 5000 rpm to use for scanning electron microscopy (SEM). The supernatant was removed and the cell pellet that was re-suspended in 60% ethanol for 1 h at 8 °C to strip off the outer cell membrane. The cells were pelleted by centrifugation and re-suspended in filtered sea water for 30 min at 8 °C. Cell pellets were re-suspended and fixed with 2.5% glutaraldehyde prepared with f/2-Si medium for 3 h at 8 °C. Cell pellets were washed twice

with f/2-Si medium and fixed overnight at 8 °C with 2% OsO_4 made up with filtered sea water. The supernatant was removed and the cell pellet was allowed to adhere to a coverslip coated with poly-L-lysine (molecular weight 70,000–150,000). The attached cells were washed for 10 min in a 1:1 solution of distilled water and filtered sea water, followed by a second wash in distilled water lasting 10 min. The samples were then dehydrated in a series of ethanol (10, 30, 50, 70, 90 and 3× in 100%, 10 min at each step), critical point dried (K850 Critical Point Dryer, Quorum/Emitech, West Sussex, UK), sputter-coated with gold, and examined with a Zeiss Sigma FE (Carl Zeiss Inc., Oberkochen, Germany) scanning electron microscope.

2.4. PCR amplifications and sequencing

The total algal DNA was extracted from 10 mL of exponentially growing *Azadinium* cultures using a plant DNA extraction kit (Sangon, Shanghai, China) according to the manufacturer's protocol. PCR amplifications were carried out using 1× PCR buffer, 50 μM dNTP mixture, 0.2 μM of each primer, 10 ng of template genomic DNA, and 1 U of ExTaq DNA Polymerase (Takara, Tokyo, Japan) in 50 μL total volume reactions. The total ITS1–5.8S–ITS2 was amplified using ITSA and ITSB primers (Adachi et al., 1996). Approximately 1400 bp of the LSU rDNA (D1–D6) was amplified using the primers of D1R (Scholin et al., 1994) and 28-1483R (Daugbjerg et al., 2000). The PCR protocol was as follows: initial denaturation for 3.5 min at 94 °C, followed by 35 cycles of 50 s denaturation at 94 °C, 50 s annealing at 45 °C, and 80 s extension at 72 °C, plus a final extension of 10 min at 72 °C. PCR products were sequenced directly in both directions using the ABI Big-Dye dye-terminator technique (Applied Biosystems, Foster City, CA, USA), according to the manufacturer's recommendations. New sequences were deposited in the GenBank with accession numbers KU686475 and KU686476.

2.5. Sequence alignment and phylogenetic analysis

Newly obtained LSU rDNA and ITS sequences of *Azadinium poporum* were aligned with the related sequences download from GenBank using the MAFFT v7.110 (Katoh et al., 2005) online program (http://mafft.cbrc.jp/alignment/server/). Alignments were manually checked with BioEdit v. 7.0.5 (Hall, 1999). The program Jmodeltest (Posada, 2008) was used to select the most appropriate model of molecular evolution with the Akaike information criterion (AIC). This test chose the TIM1 + I + G and TIM2 + G models for LSU and ITS, respectively. A Bayesian reconstruction of the data matrix was performed with MrBayes 3.1.2 (Ronquist and Huelsenbeck, 2003) using the best-fitting substitution model. Four Markov chain Monte Carlo (MCMC) chains ran for one million generations, with sampling every 1000 generations. A majority rule consensus tree was created to examine the posterior probabilities of each clade. The maximum-likelihood (ML) analyses were conducted using RaxML v7.2.6 (Stamatakis, 2006) on the T-REX web server (Boc et al., 2012) using the model GTR+G. Node support was assessed with 1000 bootstrap replicates.

2.6. Chemical analysis of azaspiracids

Cultures of *Azadinium poporum* were grown in 200 mL Erlenmeyer flasks under standard culture conditions to conduct an AZA analysis. About 10^7 cells were collected by centrifugation at the exponential phase. Cell pellets were extracted with 300 μL acetone by reciprocal shaking at 6.5 m s^{-1} with 0.9 g lysing matrix D (Thermo Savant, Illkirch, France) in a Bio101 FastPrep instrument (Thermo Savant, Illkirch, France) for 45 s. The extracts were then centrifuged (Eppendorf 5415 R, Hamburg, Germany) at 16,100 × *g* at 4 °C for 15 min. Each supernatant was transferred to a 0.45-μm pore-size spin-filter (Millipore Ultrafree, Eschborn, Germany) and centrifuged for 30 s at 800 × *g*, and the resulting filtrate was transferred into an LC autosampler vial for LC–MS/MS analysis.

2.6.1. Single reaction monitoring (SRM) measurements

Water was deionized and purified (Milli-Q, Millipore, Eschborn, Germany) to 18 MΩ cm^{-1} or better quality. Formic acid (90%, p.a.), acetic acid (p.a.) and ammonium formate (p.a.) were from Merck (Darmstadt, Germany). The solvents, methanol and acetonitrile, were high performance liquid chromatography (HPLC) grade (Merck, Darmstadt, Germany).

Mass spectral experiments were performed to survey for a wide array of AZAs. The analytical system consisted of an AB-SCIEX-4000 Q Trap, triple quadrupole mass spectrometer equipped with a TurboSpray® interface coupled to an Agilent model 1100 LC. The LC equipment included a solvent reservoir, in-line degasser (G1379A), binary pump (G1311A), refrigerated autosampler (G1329A/G1330B), and temperature-controlled column oven (G1316A).

Separation of AZAs (5 μL sample injection volume) was performed by reverse-phase chromatography on a C8 phase. The analytical column (50 mm × 2 mm) was packed with 3 μm Hypersil BDS 120 Å (Phenomenex, Aschaffenburg, Germany) and maintained at 20 °C. The flow rate was 0.2 mL min^{-1} and gradient elution was performed with two eluants, wherein eluant A was water and B was acetonitrile/water (95:5, v/v), and both contained 2.0 mM ammonium formate and 50 mM formic acid. The initial conditions were 8 min column equilibration with 30% B, followed by a linear gradient to 100% B in 8 min, isocratic elution until 18 min with 100% B, and then returning to the initial conditions until 21 min (total run time: 29 min).

The AZA profiles were determined in one period (0–18) min with curtain gas: 10 psi, CAD: medium, ion spray voltage: 5500 V, ambient temperature; nebulizer gas at 10 psi, auxiliary gas was off, the interface heater was on, the declustering potential @ 100 V, the entrance potential @ 10 V, and the exit potential @ 30 V. The SRM experiments were carried out in positive ion mode by selecting the transitions shown in Table 1. AZAs were calibrated against an external standard solution of AZA-2 (certified reference material (CRM) program of the IMB-NRC, Halifax, Canada) and expressed as AZA-2 equivalents.

Table 1
Mass transitions *m/z* (Q1 > Q3 mass) and their respective AZAs.

Mass transition	Toxin	Collision energy (CE) [V]
716 > 698	AZA-33	40
816 > 798	AZA-39	40
816 > 348	AZA-39	70
828 > 658	AZA-3	70
828 > 810	AZA-3	40
830 > 812	AZA-38	40
830 > 348	AZA-38	70
842 > 672	AZA-1	70
842 > 824	AZA-1, AZA-40	40
844 > 826	AZA-4, AZA-5	40
846 > 828	AZA-37	40
856 > 672	AZA-2	70
856 > 838	AZA-2	40
858 > 840	AZA-7, AZA-8, AZA-9, AZA-10, AZA-36	40
868 > 362	Undescribed	70
870 > 852	Me-AZA-2	40
872 > 854	AZA-11, AZA-12	40
936 > 918	AZA-2 phosphate	40

2.6.2. Precursor ion experiments

Precursors of the fragments *m/z* 348, *m/z* 360 and *m/z* 362 were scanned in the positive ion mode from *m/z* 400 to 950 under the following conditions: curtain gas at 10 psi, CAD at medium, ion spray voltage at 5500 V, ambient temperature, a 10 psi nebulizer gas, the auxiliary gas was off, the interface heater was on, a declustering potential of 100 V, a 10 V entrance potential, a 70 V collision energy, and a 12 V exit potential.

2.6.3. Collision Induced Dissociation (CID) spectra

CID spectra of *m/z* 856 and *m/z* 936 were recorded in the Enhanced Product Ion (EPI) mode in the mass range from *m/z* 150 to 960 in a positive ionization and unit resolution mode. The following parameters were applied: 10 psi curtain gas, medium CAD, a 5500 V ion spray voltage, ambient temperature, a 10 psi nebulizer gas, the auxiliary gas was off, the interface heater was on, there was a 100 V declustering potential, the collision energy spread was 0 and 10 V, and the collision energy was 70 V.

3. Results

3.1. Morphology

The cells of *Azadinium poporum* strain GM29 were 11.2–16.0 μm long (mean = 13.3 ± 1.2 μm, *n* = 30) and 8.2–11.8 μm wide (mean = 9.8 ± 0.9 μm, *n* = 30) with a median length: width ratio of around 1.4. The large nucleus was spherical to slightly elongated and located in the lower part of the cell (Fig. 1). Up to three pyrenoids were visible in the light microscope, and were located either in the epitheca or hypotheca (Fig. 1A). A single chloroplast was situated in the periphery of the cell (Fig. 1B).

The cells had a conical epitheca and a hemispherical hypotheca, interrupted by a deep and wide cingulum, descending less than half the cingulum width (Fig. 2A). Trichocysts were observed on the cell surface, including the cingular and sulcal plates. The cells showed a plate pattern of po, cp, x, 4′, 3a, 6″, 6C, 5S, 6‴, 2⁗. The cingulum was composed out of six plates of similar size (Fig. 2A and B). The rounded apical pore was located in the center of a pore plate (po) and covered by a cover plate (cp) (Fig. 2C). There was a distinct ventral pore (vp) located at the junction of the apical pore and the first two apical plates (1′, 2′) (Fig. 2C). The first apical plate was not symmetrical (Fig. 2C). There were three anterior intercalary plates (1a, 2a and 3a) on the dorsal part of the epitheca. Plates 1a and 3a were pentagonal or hexagonal, much larger than the four-sided 2a (Fig. 2B and D). The first precingular plate was large and in contact with Plate 1a (Fig. 2D). The first antapical plate (1⁗) was much smaller than the second antapical plate and displaced to the left (Fig. 2E). The sulcus was composed of an anterior sulcal plate (Sa), a median sulcal plate (Sm), a right sulcal plate (Sd), a left sulcal plate (Ss), and a posterior sulcal plate (Sp) (Fig. 2F). There was a distinct group of pores located on the dorsal side of the second antapical plate, where 10–23 pores were arranged in short rows (Fig. 2G). Cells with aberrant plate patterns (e.g., five apical plates, two anterior intercalary plate, five postcingular plates) were observed in the same culture (Fig. S1).

Supplementary Fig. S1 related to this article can be found, in the online version, at doi:10.1016/j.hal.2016.02.006.

3.2. Molecular analysis and phylogeny

For the LSU sequences, the similarity among the different ribotypes of *Azadinium poporum* ranged from 95.4% to 98.2% and the genetic distances ranged from 0.02 to 0.04. In contrast, the similarity and genetic distances were around 93% and 0.07 at interspecific level (Table 2). For the ITS sequences, the similarity among the different ribotypes of *A. poporum* ranged from 97.1% to 99.2%, and the genetic distances ranged from 0.01 to 0.02. In contrast, at the interspecific level, the similarity and genetic distances were around 91% and 0.08 (Table 3).

The ML and BI analysis that are based on LSU sequences generated similar phylogenetic trees (Fig. 3). Both *Azadinium* and *A. poporum* were monophyletic with maximal support (bootstrap = 100% in ML and pp = 1.00 in BI, respectively). *A. poporum* comprised 3 well-supported clades, referred to as ribotype A, B, and C. The strain GM29 was a sister clade of ribotype C with strong support (bootstrap = 100% in ML and pp = 0.99 in BI, respectively).

The ML and BI analysis based on ITS sequences generated similar phylogenetic trees (Fig. 4). *Azadinium poporum* comprised three well-supported clades, referred to as ribotype A, B, and C. The strain GM29 was a sister clade of ribotype B with maximal support. GM29 belonged to neither ribotype B nor ribotype C and was thus designated as a new ribotype, termed as ribotype D.

3.3. AZA profile

Precursor ion experiments of the typical AZA fragments *m/z* 348, *m/z* 360 and *m/z* 362 were performed to test the presence of AZAs. Whereas the *m/z* 348 and the *m/z* 360 experiments were negative, the *m/z* 362 experiment resulted in two peaks with *m/z* 856 at a retention time of 12.4 min and *m/z* 936 at 11.5 min. The CID spectra of both masses were recorded and resulted in identical spectra to those of AZA-2 and AZA-2 phosphate (Fig. 5). Quantification of both compounds against an external calibration solution of AZA-2 in the Selected Reaction Monitoring (SRM) mode gave an AZA-2 cell quota of 45 ± 1 fg cell^{-1}. AZA-2 phosphate was expressed as AZA-2 equivalent and determined as 0.7 ± 0.5 fg cell^{-1}.

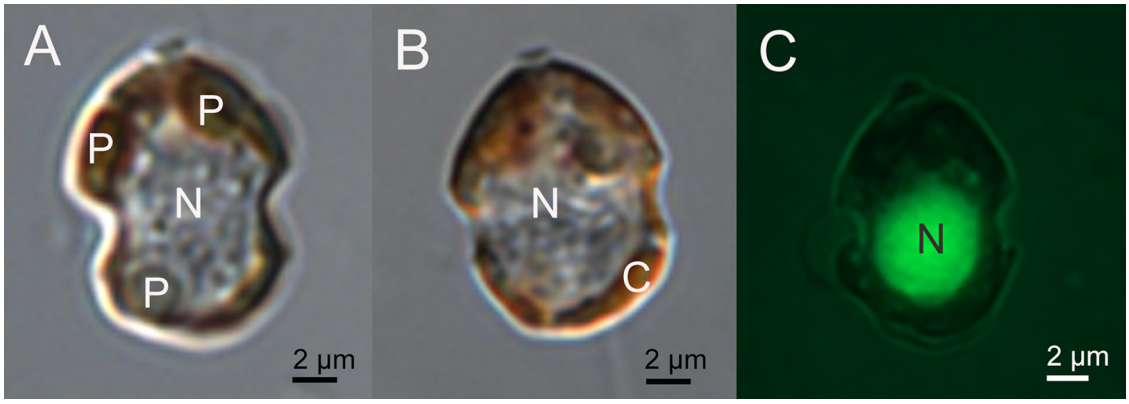

Fig. 1. LM of live cells of *Azadinium poporum* strain GM29. (A) Ventral view, showing a large nucleus (N) and several pyrenoids (P). (B) Ventral view, showing a putative large chloroplast. (C) Ventral view, showing a large nucleus (Sybr Green staining).

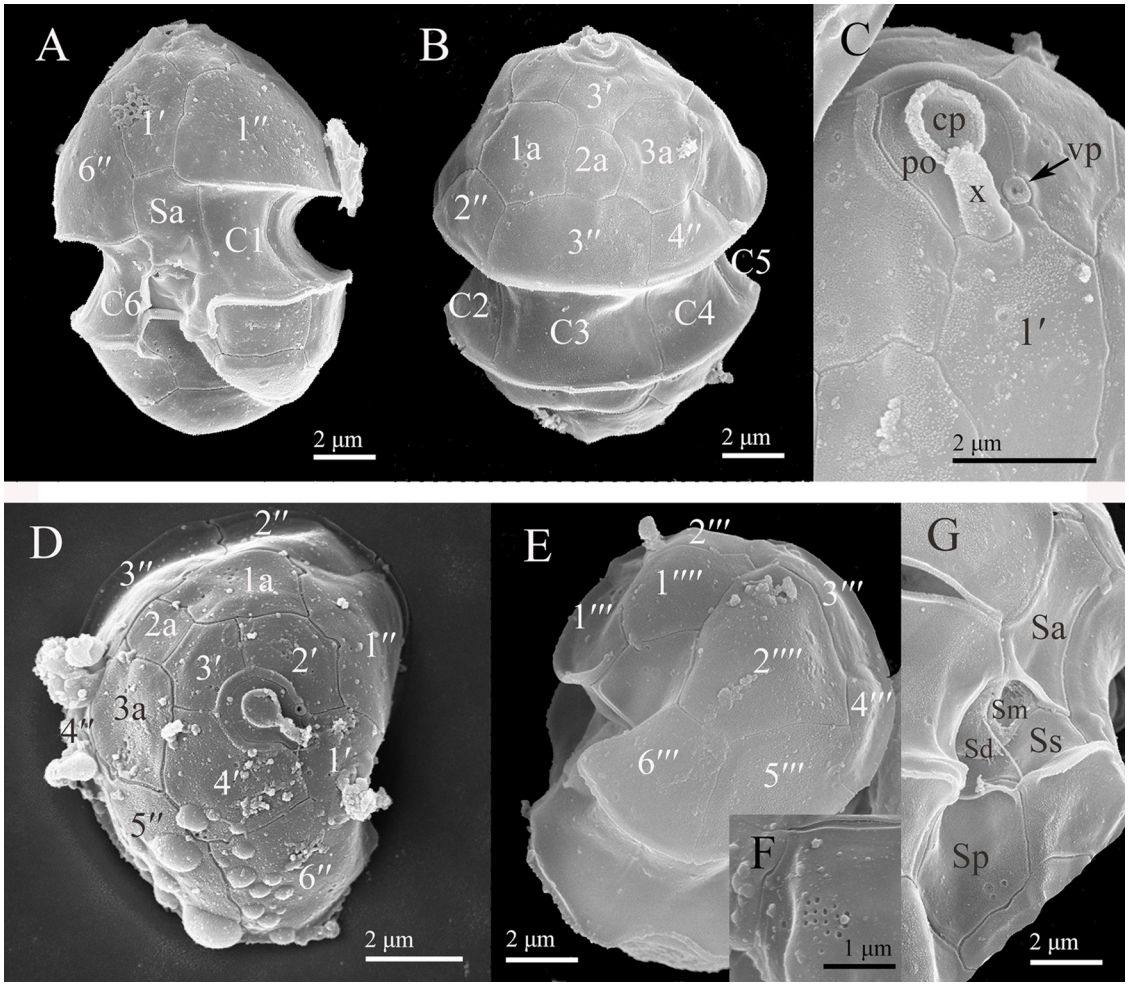

Fig. 2. A scanning electron micrograph of vegetative cells of *Azadinium poporum* strain GM29. (A) Ventral view, showing the conical epitheca and round hypotheca. (B) Dorsal view, showing three anterior intercalary plates (1a–3a). (C) Apical view, showing the first apical plate (1′), pore plate (po), cover plate (cp) and ventral pore (vp). (D) Apical view, showing four apical plates (1′–4′), three intercalary plates and six precingular plates (1″–6″). (E) Antapical view, showing six postcingular plates (1‴–6‴) and two antapical plates (1⁗ and 2⁗) of unequal size. (F) Detail of plate 2⁗, showing a group of pores on the dorsal side. (G) Sulcal plates, showing an anterior sulcal plate (Sa), a median sulcal plate (Sm), a right sulcal plate (Sd), a left sulcal plate (Ss), and a posterior sulcal plate (Sp).

Table 2
Partial LSU sequences comparison of *Azadinium poporum* strain GM29 from the Gulf of Mexico with those of related species from elsewhere. The percentage refers to the similarity out of partial LSU sequences (701 bp); the numeral in brackets refers to pairwise genetic distance.

	GM29	G25	G66	G42	UTHC5	AZCH02
GM29 (ribotype D)	–					
G25 (ribotype B)	97.7% (0.02)	–				
G66 (ribotype B)	97.8% (0.02)	98.2% (0.02)	–			
G42 (ribotype C)	98.2% (0.02)	97.7% (0.02)	97.5% (0.02)	–		
UTHC5 (ribotype A)	95.4% (0.04)	96.2% (0.04)	96.4% (0.03)	96.5% (0.03)	–	
AZCH02 (*A. dalianense*)	92.7% (0.07)	91.7% (0.08)	92.2% (0.07)	93.2% (0.06)	92.7% (0.06)	–

Table 3
ITS sequences comparison of *Azadinium poporum* strain GM29 from the Gulf of Mexico with those of related species from elsewhere. The percentage refers to the similarity out of ITS region sequences; the numeral in bracket refers to pairwise genetic distance.

	GM29	G25	G66	G42	UTHC5	AZCH02
GM29 (ribotype D)	–					
G25 (ribotype B)	98.8% (0.01)	–				
G66 (ribotype B)	98.7% (0.01)	99.2% (0.01)	–			
G42 (ribotype C)	98.4% (0.02)	98.2% (0.02)	97.7% (0.02)	–		
UTHC5 (ribotype A)	97.6% (0.02)	97.3% (0.02)	97.1% (0.02)	97.3% (0.02)	–	
AZCH02 (*A. dalianense*)	90.8% (0.08)	90.6% (0.08)	90.8% (0.08)	90.6% (0.08)	91.3% (0.08)	–

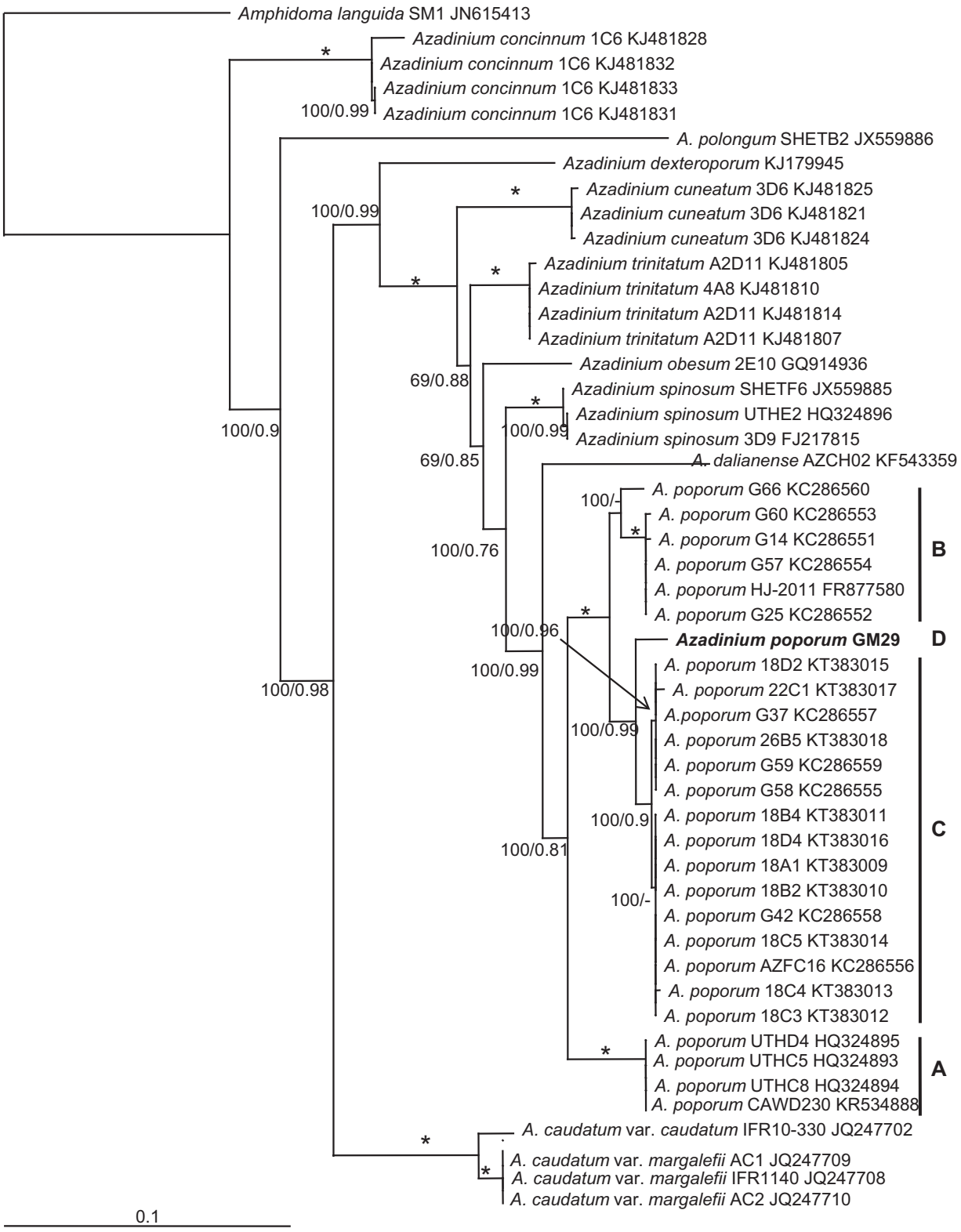

Fig. 3. Phylogeny of *Azadinium poporum* inferred from partial LSU rDNA sequences using maximum likelihood (ML). Branch lengths are drawn to scale, with the scale bar indicating the number of nucleotide substitutions per site. Numbers on branches are statistical support values to clusters on the right of them (left: ML bootstrap support values; right: Bayesian posterior probabilities).

4. Discussion

4.1. Morphology and biogeography

This is the first report of the toxic genus *Azadinium* in waters of the United States. In contrast to the high diversity of *Azadinium* in Europe (up to 9 species) (Tillmann et al., 2009, 2014), there are only a few species recovered in Asian waters (*A. poporum*, *A. dalianense*) (Gu et al., 2013; Luo et al., 2013), Argentinean waters (*A.* cf. *spinosum*, *A. poporum* (Akselman and Negri, 2012; Tillmann et al., 2016), the Mexican Pacific (*A. spinosum*) (Hernández-Becerril et al., 2012), and New Zealand waters (*A. poporum*) (Smith et al., 2015),

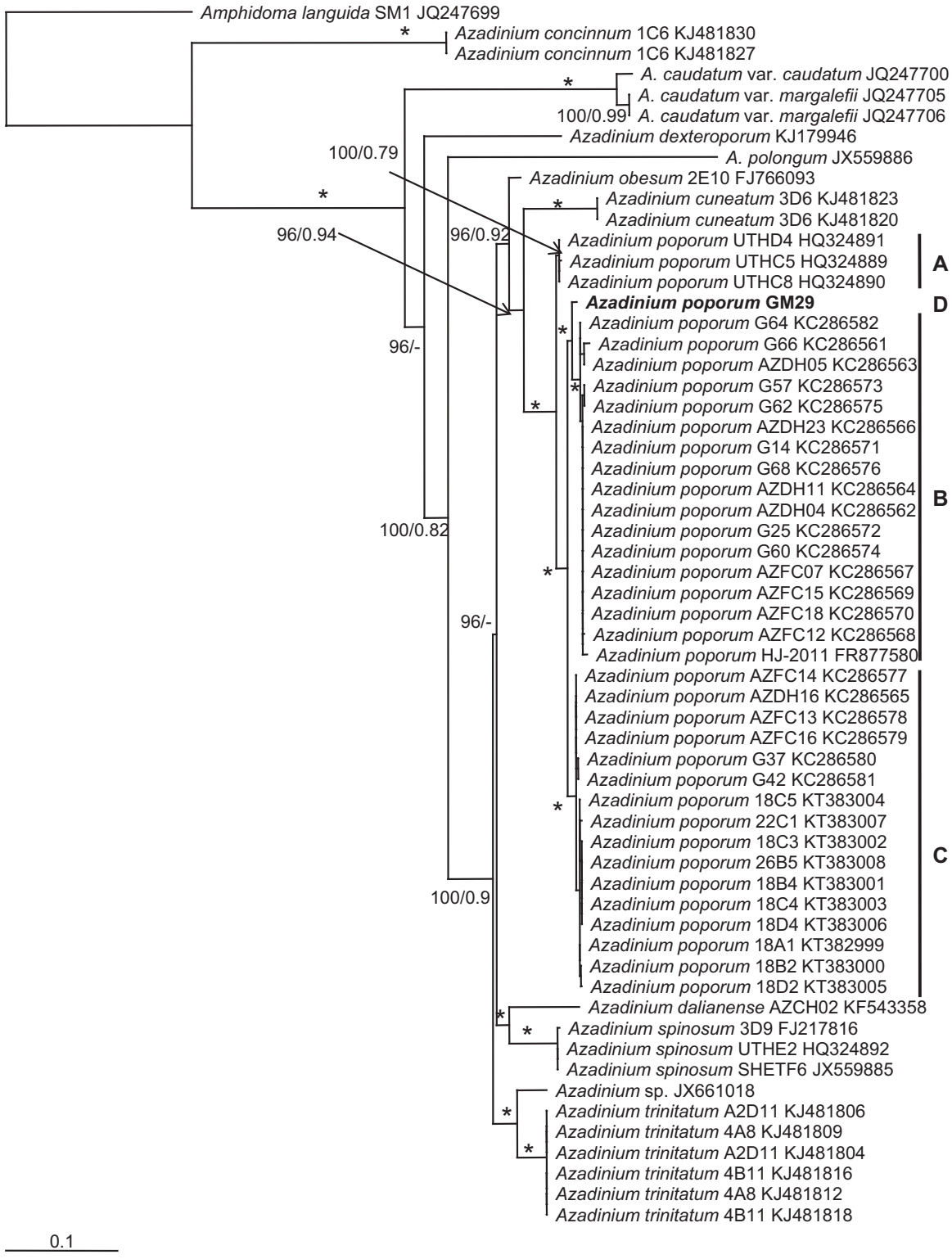

Fig. 4. Phylogeny of *Azadinium poporum* inferred from ITS and 5.8S rDNA sequences using maximum likelihood (ML). Branch lengths are drawn to scale, with the scale bar indicating the number of nucleotide substitutions per site. Numbers on branches are statistical support values to clusters on the right of them (left: ML bootstrap support values; right: Bayesian posterior probabilities).

probably because they are small and are not included in most routine monitoring. *A. poporum* seems to be the most widely distributed species with reports from the northeast Atlantic (Tillmann et al., 2010), the northwest Pacific (Potvin et al., 2011; Gu et al., 2013), southwest Atlantic (Argentina, Tillmann et al., 2016) and southwest Pacific (New Zealand, Smith et al., 2015). These species require more attention because of their toxicity, which causes azaspiracid shellfish poisoning (AZP). This occurred through consumption of AZA contaminated mussels that were cultured in Ireland and consumed in several other countries (Satake et al., 1998; Twiner et al., 2008; Klontz et al., 2009). But, as in many countries, the mouse bioassay is still used for seafood

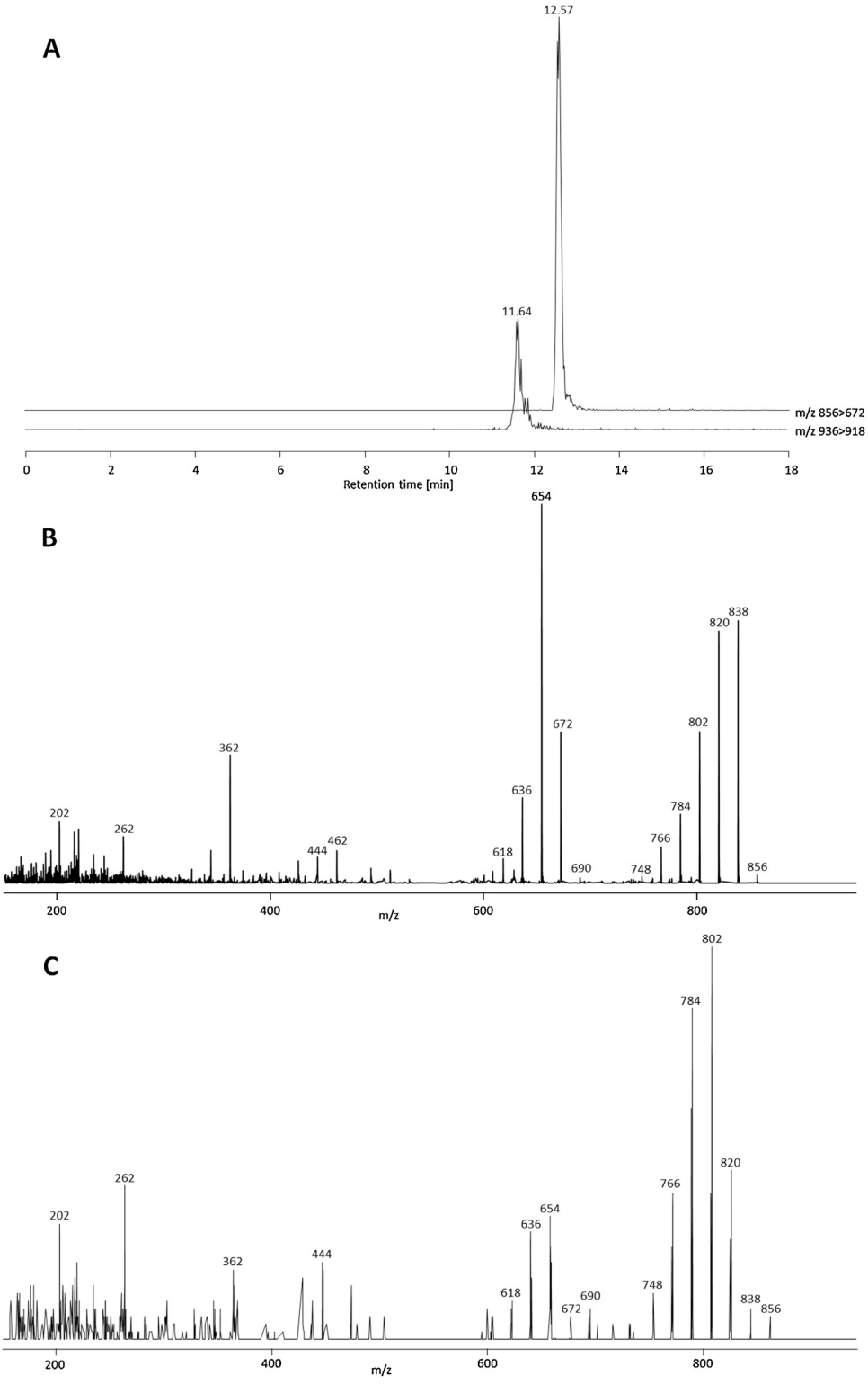

Fig. 5. (A) Selected ion traces of *Azadinium poporum* strain GM029: *m/z* 856 > 672 for AZA-2 and *m/z* 936 > 918 for AZA-2 phosphate. (B) Collision induced dissociation (CID) spectrum of *m/z* 856 (AZA-2). (C) CID spectrum of *m/z* 936 (AZA-2 phosphate).

control, and azaspiracid shellfish poisoning may have been misidentified as diarrhetic shellfish poisoning (DSP) because the symptoms of both poisonings in mice are the same. Only mass spectral analysis of contaminated shellfish can discriminate between AZP and DSP events. Therefore, insufficient attention has been paid to this group of dinoflagellates in other areas and higher diversities can be expected to be found in the near future.

The key morphological characters of the genus *Azadinium* include the presence/absence of an antapical spine, the arrangement of the first precingular plate (whether in contact with the first anterior intercalary plate or not), and the location of the ventral pore (Tillmann et al., 2014). The distinct position of the ventral pore located at the junction of the pore plate and the first two apical plates is characteristic of *Azadinium poporum*

(Tillmann et al., 2011), but such a kind of ventral pore was also observed in *Azadinium dalianense* and *Azadinium trinitatum* (Luo et al., 2013; Tillmann et al., 2014). *A. dalianense* has only three apical plates and two anterior intercalary plates (Luo et al., 2013), whereas *A. trinitatum* shares an identical plate pattern with that of *A. poporum* (Tillmann et al., 2014). However, *A. trinitatum* has an antapical spine and the left side of the suture po/1′ is farther away from the apical pore than *A. poporum*. Based on the location of the ventral pore and the absence of an antapical spine and configuration of Plate 1″, the strain GM29 can be safely classified as *A. poporum*. A group of pores on the dorsal side of the second antapical plate was observed in the Gulf of Mexico strain, which was likewise present in a Korea strain (ribotype B) (Potvin et al., 2011), and many Argentinean and Chinese strains (ribotype C) (Tillmann et al., 2016; Gu personal observations), suggesting that this is a common feature of *A. poporum* although it was not mentioned in the original description. The strain GM29 was obtained by incubating surface sediments from the Gulf of Mexico directly, supporting the idea that *A. poporum* has a cyst stage (Gu et al., 2013), although there was no direct observation of such a cyst. The cysts might be too small, too inconspicuous and rare, thus escaping microscopic detection during routine plankton surveys and cyst studies so far. In line with previously observations (Gu et al., 2013; Tillmann et al., 2011), the Gulf of Mexico strain *A. poporum* cells also sometimes show aberrant plate patterns in culture.

Before this study, *Azadinium poporum* was reported in the North Sea (ribotype A), Yellow Sea, East China Sea, South China Sea (ribotype B, C), New Zealand (ribotype A) and Argentina (ribotype C) (Tillmann et al., 2011, 2016; Gu et al., 2013; Smith et al., 2015). The distribution of *A. poporum* is extended to the Gulf of Mexico, suggesting that this is a widespread species. *A. poporum* of various ribotypes share identical thecate morphology, are relevant to toxicity, and thus highlight the necessity to develop molecular-based assays for targeting all ribotypes.

4.2. Phylogeny and genetic differentiation

The results support the monophyly of the genus *Azadinium* and *A. poporum* (Gu et al., 2013; Tillmann et al., 2014). However, the phylogenetic position of *A. poporum* strain GM29 is not consistent, and forms a sister clade either to ribotype B (LSU) or ribotype C (ITS), whereas phylogenetic positions of other strains of *A. poporum* are consistent. Thus GM29 was recognized as a new ribotype. More ribotypes can be expected as still limited sequences from a few geographical areas are available for this species. Unlike other dinoflagellates, the genetic distances of LSU rDNA among *A. poporum* ribotypes are greater than those of ITS sequences (Tables 2 and 3), supporting the idea that LSU is a better fragment for molecular discrimination (Toebe et al., 2013). However, whether the primers and probes for European *A. poporum* are also applicable for other ribotypes remains to be confirmed.

4.3. Toxin profiles

AZAs have been reported in shellfish of Pacific USA origin, but no details were provided (Trainer et al., 2013). AZA-2 was found in three plankton samples collected in Washington State (northeast Pacific), although neither AZA-1 nor AZA-3 were detected there (Trainer et al., 2013). AZA-1 was the dominant toxin profile in plankton samples collected in the North Sea (Krock et al., 2009), which was later ascribed to *Azadinium spinosum* (Tillmann et al., 2009). For all available *A. spinosum* strains, AZA-2 is present only in conjunction with AZA-1 (Tillmann et al., 2009, 2012b). For the potential toxic *Azadinium dexteroporum*, abundance of azaspiracid is very low and neither AZA-1 nor AZA-2 were produced (Percopo et al., 2013). *A. poporum* is the only known *Azadinium* species producing exclusively or predominantly AZA-2 (Krock et al., 2014; Tillmann et al., 2016; present study), thus it is likely responsible for the toxin from the plankton sample collected in Washington State (Trainer et al., 2013). AZAs were also present in shellfish from eastern Canada (Twiner et al., 2008), suggesting that toxic species (e.g., *A. poporum*, A. *spinosum*) might be present there too. In addition, the toxin profile of the *A. poporum* isolate from the Gulf of Mexico is identical with the profile of *A. poporum* from Argentinean shelf waters including the recently discovered AZA-2 phosphate (Tillmann et al., 2016), even though both isolates belong to different ribotypes: C (Argentinean isolate) and D (Gulf of Mexico isolate). In contrast, only AZA-1 was detected in mussels collected from Baja California, Mexico (García-Mendoza et al., 2014), consistent with the fact that *A. spinosum* is present in the Mexican Pacific (Hernández-Becerril et al., 2012). Interestingly, shellfish samples from Morocco (Taleb et al., 2006) and Portugal (Vale et al., 2008) show an AZA-profile with predominant AZA-2, followed by AZA-1, quite different from any shellfish sample from Ireland, Norway, Spain or France (Twiner et al., 2008). Identification of genes involved in saxitoxin biosynthesis contributed to a rapid and accurate molecular method to quantify toxic *Alexandrium* species from marine waters (Murray et al., 2011). However, AZA-related genes have not been identified yet, and their knowledge will contribute to a promising approach for monitoring and studying toxic *Azadinium* in future studies.

5. Conclusions

The first record of *Azadinium poporum* in the Gulf of Mexico supports a wide distribution of this species. Further efforts are needed to examine if it is also present in the Atlantic coast of the USA and Canada. *A. poporum* in the Gulf of Mexico is genetically different from strains from elsewhere, and thus represents a new ribotype. This strain, however, produces predominantly AZA-2 and AZA-2 phosphate, identical to the profiles produced by the Argentinean strains (Tillmann et al., 2016).

Acknowledgements

We thank Urban Tillmann and an anonymous reviewer for constructive suggestions that improved the ms. Haifeng Gu was supported by the National Natural Science Foundation of China (41376170, 41306171) and the Public Science and Technology Research Funds Projects of Ocean (201305027). Kenneth Neil Mertens was a postdoctoral fellow of FWO Belgium. Andrea M. Price was supported by a Natural Science and Engineering Research Council of Canada (NSERC) doctoral scholarship (CGS-D3). Sample collection was supported by the National Oceanic and Atmospheric Administration, Center for Sponsored Coastal Ocean Research, under award NA09NOS4780204 to Louisiana Universities Marine Consortium and award NA09NOS4780230 to Louisiana State University.[SS]

References

Adachi, M., Sako, Y., Ishida, Y., 1996. Analysis of *Alexandrium* (Dinophyceae) species using sequences of the 5.8S ribosomal DNA and internal transcribed spacer regions. J. Phycol. 32 (3), 424–432.

Akselman, R., Negri, R.M., 2012. Blooms of *Azadinium* cf. *spinosum* Elbrächter et Tillmann (Dinophyceae) in northern shelf waters of Argentina, Southwestern Atlantic. Harmful Algae 19, 30–38.

Boc, A., Diallo, A.B., Makarenkov, V., 2012. T-REX: a web server for inferring, validating and visualizing phylogenetic trees and networks. Nucleic Acids Res. 40 (W1), W573–W579.

Daugbjerg, N., Hansen, G., Larsen, J., Moestrup, Ø., 2000. Phylogeny of some of the major genera of dinoflagellates based on ultrastructure and partial LSU rDNA sequence data, including the erection of three new genera of unarmoured dinoflagellates. Phycologia 39 (4), 302–317.

García-Mendoza, E., Sánchez-Bravo, Y.A., Turner, A., Blanco, J., O'Neil, A., Mancera-Flores, J., Pérez-Brunius, P., Rivas, D., Almazán-Becerril, A., Peña-Manjarrez, J.L., 2014. Lipophilic toxins in cultivated mussels (*Mytilus galloprovincialis*) from Baja California, Mexico. Toxicon 90, 111–123.

Gu, H., Luo, Z., Krock, B., Witt, M., Tillmann, U., 2013. Morphology, phylogeny and azaspiracid profile of *Azadinium poporum* (Dinophyceae) from the China Sea. Harmful Algae 21–22, 64–75.

Guillard, R.R.L., Ryther, J.H., 1962. Studies of marine planktonic diatoms. I. *Cyclotella nana* Hustedt and *Detonula confervacea* Cleve. Can. J. Microbiol. 8 (2), 229–239.

Hall, T.A., 1999. BioEdit: a user-friendly biological sequence alignment editor and analysis program for Windows 95/98/NT. Nucleic Acids Symp. Ser. 41, 95–98.

Hernández-Becerril, D.U., Barón-Campis, S.A., Escobar-Morales, S., 2012. A new record of *Azadinium spinosum* (Dinoflagellata) from the tropical Mexican Pacific. Rev. Biol. Mar. Oceanogr. 47 (3), 553–557.

Katoh, K., Kuma, K., Toh, H., Miyata, T., 2005. MAFFT version 5: improvement in accuracy of multiple sequence alignment. Nucleic Acids Res. 33 (2), 511–518.

Klontz, K.C., Abraham, A., Plakas, S.M., Dickey, R.W., 2009. Mussel-associated azaspiracid intoxication in the United States. Ann. Intern. Med. 150 (5), 361.

Krock, B., Tillmann, U., John, U., Cembella, A.D., 2009. Characterization of azaspiracids in plankton size-fractions and isolation of an azaspiracid-producing dinoflagellate from the North Sea. Harmful Algae 8 (2), 254–263.

Krock, B., Tillmann, U., Witt, M., Gu, H., 2014. Azaspiracid variability of *Azadinium poporum* (Dinophyceae) from the China Sea. Harmful Algae 36, 22–28.

Lopez-Rivera, A., O'Callaghan, K., Moriarty, M., O'Driscoll, D., Hamilton, B., Lehane, M., James, K., Furey, A., 2010. First evidence of azaspiracids (AZAs): a family of lipophilic polyether marine toxins in scallops (*Argopecten purpuratus*) and mussels (*Mytilus chilensis*) collected in two regions of Chile. Toxicon 55 (4), 692–701.

Luo, Z., Gu, H., Krock, B., Tillmann, U., 2013. *Azadinium dalianense*, a new dinoflagellate species from the Yellow Sea, China. Phycologia 52 (6), 625–636.

Murray, S.A., Wiese, M., Stüken, A., Brett, S., Kellmann, R., Hallegraeff, G., Neilan, B.A., 2011. sxtA-based quantitative molecular assay to identify saxitoxin-producing harmful algal blooms in marine waters. Appl. Environ. Microbiol. 77 (19), 7050–7057.

Nézan, E., Tillmann, U., Bilien, G., Boulben, S., Chèze, K., Zentz, F., Salas, R., Chomérat, N., 2012. Taxonomic revision of the dinoflagellate *Amphidoma caudata*: transfer to the genus *Azadinium* (Dinophyceae) and proposal of two varieties, based on morphological and molecular phylogenetic analyses. J. Phycol. 48 (4), 925–939.

Percopo, I., Siano, R., Rossi, R., Soprano, V., Sarno, D., Zingone, A., 2013. A new potentially toxic *Azadinium* species (Dinophyceae) from the Mediterranean Sea, *A. dexteroporum* sp. nov. J. Phycol. 49 (5), 950–966.

Posada, D., 2008. jModelTest: phylogenetic model averaging. Mol. Biol. Evol. 25 (7), 1253–1256.

Potvin, É., Jeong, H.J., Kang, N.S., Tillmann, U., Krock, B., 2011. First report of the photosynthetic dinoflagellate genus *Azadinium* in the Pacific Ocean: morphology and molecular characterization of *Azadinium* cf. *poporum*. J. Eukaryot. Microbiol. 59 (2), 145–156.

Ronquist, F., Huelsenbeck, J.P., 2003. MrBayes 3: Bayesian phylogenetic inference under mixed models. Bioinformatics 19 (12), 1572–1574.

Satake, M., Ofuji, K., Naoki, H., James, K.J., Furey, A., McMahon, T., Silke, J., Yasumoto, T., 1998. Azaspiracid, a new marine toxin having unique spiro ring assemblies, isolated from Irish mussels, *Mytilus edulis*. J. Am. Chem. Soc. 120 (38), 9967–9968.

Scholin, C.A., Herzog, M., Sogin, M., Anderson, D.M., 1994. Identification of group- and strain-specific genetic markers for globally distributed *Alexandrium* (Dinophyceae). II. Sequence analysis of a fragment of the LSU rRNA gene. J. Phycol. 30 (6), 999–1011.

Smith, K.F., Rhodes, L., Harwood, D.T., Adamson, J., Moisan, C., Munday, R., Tillmann, U., 2015. Detection of *Azadinium poporum* in New Zealand: the use of molecular tools to assist with species isolations. J. Appl. Phycol., http://dx.doi.org/10.1007/s10811-015-0667-5.

Stamatakis, A., 2006. RAxML-VI-HPC: maximum likelihood-based phylogenetic analyses with thousands of taxa and mixed models. Bioinformatics 22 (21), 2688–2690.

Taleb, H., Vale, P., Amanhir, R., Benhadouch, A., Sagou, R., Chafik, A., 2006. First detection of azaspiracids in mussels in north west Africa. J. Shellfish Res. 25 (3), 1067–1070.

Tillmann, U., Elbrächter, M., Krock, B., John, U., Cembella, A., 2009. *Azadinium spinosum* gen. et sp. nov. (Dinophyceae) identified as a primary producer of azaspiracid toxins. Eur. J. Phycol. 44 (1), 63–79.

Tillmann, U., Elbrächter, M., John, U., Krock, B., Cembella, A., 2010. *Azadinium obesum* (Dinophyceae), a new nontoxic species in the genus that can produce azaspiracid toxins. Phycologia 49 (2), 169–182.

Tillmann, U., Elbrächter, M., John, U., Krock, B., 2011. A new non-toxic species in the dinoflagellate genus *Azadinium*: *A. poporum* sp. nov. Eur. J. Phycol. 46 (1), 74–87.

Tillmann, U., Salas, R., Gottschling, M., Krock, B., O'Driscoll, D., Elbrächter, M., 2012a. *Amphidoma languida* sp. nov. (Dinophyceae) reveals a close relationship between *Amphidoma* and *Azadinium*. Protist 163 (5), 701–719.

Tillmann, U., Soehner, S., Nézan, E., Krock, B., 2012b. First record of the genus *Azadinium* (Dinophyceae) from the Shetland Islands, including the description of *Azadinium polongum* sp. nov. Harmful Algae 20, 142–155.

Tillmann, U., Gottschling, M., Nézan, E., Krock, B., Bilien, G., 2014. Morphological and molecular characterization of three new *Azadinium* species (Amphidomataceae, Dinophyceae) from the Irminger Sea. Protist 165 (4), 417–444.

Tillmann, U., Borel, C.M., Barrera, F., Lara, R., Krock, B., Almandoz, G.O., Witt, M., Trefault, N., 2016. *Azadinium poporum* from the Argentine continental shelf, southwestern Atlantic, produces azaspiracid-2 and azaspiracid-2 phosphate. Harmful Algae 51, 40–55.

Toebe, K., Joshi, A.R., Messtorff, P., Tillmann, U., Cembella, A., John, U., 2013. Molecular discrimination of taxa within the dinoflagellate genus *Azadinium*, the source of azaspiracid toxins. J. Plankton Res. 35 (1), 225–230.

Trainer, V.L., Moore, L., Bill, B.D., Adams, N.G., Harrington, N., Borchert, J., Da Silva, D.A., Eberhart, B.T.L., 2013. Diarrhetic shellfish toxins and other lipophilic toxins of human health concern in Washington State. Mar. Drugs 11 (6), 1815–1835.

Twiner, M.J., Rehmann, N., Hess, P., Doucette, G.J., 2008. Azaspiracid shellfish poisoning: a review on the chemistry, ecology, and toxicology with an emphasis on human health impacts. Mar. Drugs 6 (2), 39–72.

Ueoka, R., Ito, A., Izumikawa, M., Maeda, S., Takagi, M., Shin-ya, K., Yoshida, M., van Soest, R.W.M., Matsunaga, S., 2009. Isolation of azaspiracid-2 from a marine sponge *Echinoclathria* sp. as a potent cytotoxin. Toxicon 53 (6), 680–684.

Vale, P., Bire, R., Hess, P., 2008. Confirmation by LC–MS/MS of azaspiracids in shellfish from the Portuguese north-western coast. Toxicon 51 (8), 1449–1456.

Yao, J., Tan, Z., Zhou, D., Guo, M., Xing, L., Yang, S., 2010. Determination of azaspiracid-1 in shellfishes by liquid chromatography with tandem mass spectrometry. Chin. J. Chromatogr. 28 (4), 363–367 (in Chinese).